Regulated Expression of Vimentin cDNA in Cells in the Presence and Absence of a Preexisting Vimentin Filament Network

Alfonso J. Sarria, Steven K. Nordeen, and Robert M. Evans

Department of Pathology, University of Colorado Health Sciences Center, Denver, Colorado 80262

Abstract. Human cells were transfected with a mouse vimentin cDNA expression vector containing the hormone response element of mouse mammary tumor virus. The distribution of mouse vimentin after induction with dexamethasone was examined by indirect immunofluorescence with antivimentin antibodies specific for either mouse or human vimentin. In stably transfected HeLa cells, which contain vimentin filaments, addition of dexamethasone resulted in the initial appearance of mouse vimentin in discrete areas, usually perinuclear, that always corresponded to areas of the human filament network with the most intense fluorescence. Within 20 h after addition of dexamethasone, the mouse and human vimentin immunofluorescence patterns were identical. However, in stably transfected MCF-7 cells, which lack vimentin filaments, induction of mouse vimentin synthesis resulted in assembly of vimentin filaments throughout the cytoplasm without any obvious local concentrations.

Transient expression experiments with SW-13 cell subclones that either lack or contain endogenous vimentin filaments yielded similar results to those obtained with MCF-7 and HeLa transfectants, respectively. Further experiments with HeLa transfectants were conducted to follow the fate of the mouse protein after synthesis had dropped after withdrawal of dexamethasone. The mouse vimentin-specific fluorescence was initially lost from peripheral areas of the cells while the last detectable mouse vimentin always corresponded to the human filament network with the most intense fluorescence. These studies are consistent with a uniform assembly of vimentin filaments throughout the cytoplasm and suggest that previous observations of polarized or vectorial assembly from a perinuclear area to more peripheral areas in cells may be attributable to the nonuniformly distributed appearance of vimentin filaments in immunofluorescence microscopy.

INTERMEDIATE filaments are believed to be the most stable component of the cytoskeleton of mammalian cells. Studies of the physical characteristics of the subunit proteins and subunit protein assembly have shown that intermediate filaments have properties that differ substantially from those of microtubules and microfilaments (for reviews see Steinert and Roop, 1988; Klymkowsky et al., 1989; Sarria and Evans, 1989). Unlike microfilaments and microtubules, most of the intermediate filament protein in cells is found in an insoluble, filamentous form, with only a very small fraction of the total present in a soluble form (Soellner et al., 1985). Pulse–chase studies with vimentin-type filaments have indicated that newly synthesized intermediate filament protein is first present in this small soluble pool but is then rapidly incorporated into the insoluble filaments (Blikstad and Lazarides, 1983; Soellner et al., 1985). Although these reports differ slightly concerning the degree of subsequent exchange of subunit protein between the soluble and filamentous forms, once assembled, intermediate filaments would appear to be less dynamic structures than microfilaments or microtubules.

The cytoplasmic network of intermediate filaments appears to form close associations with the nucleus and plasma membrane (Goldman et al., 1985; 1986). Although the filaments are believed to be apolar structures, some studies have raised the possibility that the assembly and dynamics of the intermediate filament network in cells may be a process with an intrinsic polarity with respect to the nucleus and plasma membrane (see Robson, 1989). Eckert et al. (1982a) initially observed that the in vitro assembly of keratin protein onto detergent-extracted epithelial cytoskeletons appeared to occur preferentially in areas of cytoplasm around the nucleus. It was also shown that antibody-induced keratin filament collapse resulted in perinuclear filament aggregates (Eckert et al., 1982b). Based on these observations and the appearance of keratin filaments in motile cells, Eckert and Caputi (1985) proposed that intermediate filaments are assembled at specific perinuclear distribution centers. Albers and Fuchs (1987) transiently expressed a truncated mutant keratin cDNA in cells that disrupted the endogenous keratin filament network. In cells recovering after this transient expression, the newly formed normal keratin filaments appeared first in a perinuclear location. In contrast, microinjection of polyadenylated RNA from epithelial cells into heterologous epithelial (Franke et al., 1984) and nonepithelial (Kreis et al., 1983) cells has been shown to result in keratin filament

assembly dispersed throughout the cytoplasm, not indicating a particular localization for filament assembly.

Observations on the assembly of modified filament proteins in cells have appeared to support the concept that intermediate assembly may take place specifically in a perinuclear location. Vikstrom et al. (1989) microinjected biotinylated vimentin into fibroblasts that contained a preexisting vimentin filament network and found that with time after injection, the modified vimentin was first detected in filaments near the nucleus and then gradually later in filaments that extended into more peripheral areas of the cytoplasm. Similarly, Albers and Fuchs (1989) transiently expressed a modified keratin cDNA in epithelial cells and reported that the modified keratin protein was detected initially in filaments at a perinuclear location and then progressively along the cytoplasmic filaments more distant from the nucleus. These studies suggested that intermediate filament assembly may take place in a perinuclear location and progress in a vectorial or polarized manner toward the cell periphery. One significant concern in the interpretation of these results involves the fact that in most cells intermediate filaments are not uniformly distributed in the cytoplasm at the level of immunofluorescence and are often seen as perinuclear accumulations. Because it might be expected that filament protein incorporated uniformly into assembled filaments would also be first detectable in immunofluorescence in areas with the highest preexisting filament concentration, it is difficult to differentiate between polarized and uniform subunit assembly on this basis.

Recently, Ngai et al. (1990) reported that expression of a chicken vimentin cDNA in mouse fibroblasts resulted in incorporation of the newly synthesized chicken vimentin into the existing mouse filament network at discrete sites throughout the cytoplasm. However, intermediate filaments are dynamic structures with a finite half-life (Albers and Fuchs, 1987; 1989). Therefore, experiments to localize newly synthesized vimentin in this background of a preexisting filament network are difficult to interpret.

These studies involve the characterization of regulatable expression of a mouse vimentin cDNA in human cells in the presence and also in the absence of a preexisting human vimentin filament network. This approach allows for not only detection of newly synthesized vimentin incorporated into assembled intermediate filaments, but also the study of
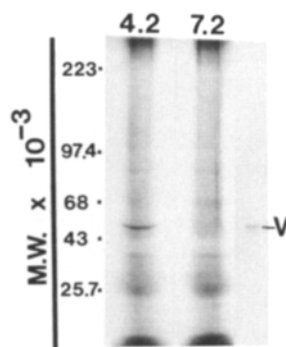
Figure 1. In vitro transcription and translation of mouse vimentin cDNA containing plasmids pFB4.2 and pFB7.2. Transcription was initiated using the phage T7 promoter. The resulting RNA was translated in a reticulocyte lysate system. The translation products were analyzed on a 7.5% SDS-polyacrylamide gel. The figure shows the [^{35}S] autoradiograph of the in vitro translated proteins separated by SDS-PAGE. The position of purified vimentin (*V*) and molecular weight standards (*Sigma SDS-6H*) are indicated.
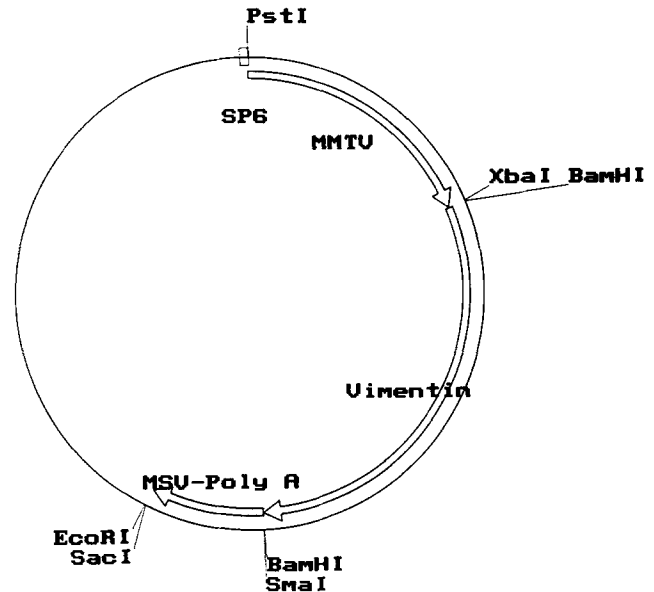
Figure 2. Map of the vimentin cDNA expression plasmid pSP64-MMTV-VimS used in transfection studies. The map gives the location of the restriction sites derived from the original pSP64 polylinker.

de novo assembly and the fate of the assembled mouse filament protein in cells after its synthesis has ceased.

Materials and Methods

Isolation of a Mouse Vimentin cDNA

Total cellular RNA was isolated from mouse L-929 cells by the guanidinium thiocyanate procedure of Han et al. (1987) and poly A+ RNA selected by oligo (dT)-cellulose chromatography. This RNA was used for DNA synthesis using a commercial cDNA synthesis kit (Pharmacia Fine Chemicals, Piscataway, NJ) to produce a recombinant library in the phagemid lambda-ZAP (Stratagene Corp., La Jolla, CA). The library was screened by replica filter hybridization using a ^{32}P-labeled hamster vimentin cDNA, pVim-1 (Quax-Jeuken et al., 1983) (gift of Dr. H. Bloemendal). A number of positive recombinants were obtained and two were selected for further study. Both were found to contain inserts of ~1.8 kb that hybridized with the pVim-1 probe (data not shown). When produced as the excised plasmid form (Bluescript SK-), the plasmids pFB4.2 and pFB7.2 yielded restriction maps indicating identical vimentin inserts in opposite orientations. Both plasmids were linearized with Xba I and the inserts transcribed in vitro using T7 RNA polymerase. The resulting RNA was then translated in a reticulocyte lysate system containing [^{35}S]methionine followed by analysis of the ^{35}S-labeled proteins by SDS-PAGE (Laemmli, 1970). Molecular weight markers from a commercial kit were used as a reference (SDS-6H; Sigma Chemical Co., St. Louis, MO). As shown in Fig. 1, pFB4.2 yielded a single labeled 57-kD protein species which comigrated with purified mouse vimentin, whereas pFB7.2 yielded only background reticulocyte proteins. A comparison of the restriction maps of pFB4.2 and pFB7.2 (not shown) with the hamster vimentin sequence (Quax et al., 1983), and the in vitro transcription/translation data indicate that pFB4.2 contained a full-length vimentin cDNA sequence in the sense orientation with respect to the T7 promoter.

Construction of Regulatable Vimentin cDNA and Glucocorticoid Receptor–Neomycin Resistance Expression Vectors

The plasmid pFB4.2 was digested with Eco RI and the excised 1.8-kb vimentin cDNA insert was purified. The ends were made flush with T4 DNA polymerase, Bam HI linkers were added, and the cDNA was inserted into the Bam HI site of the plasmid pSP64-MMTV. This plasmid is a pSP64-based plasmid containing the promoter and hormone response element of

mouse mammary tumor virus and the polyadenylation signal of murine sarcoma virus (gift of F. van der Hoorn). A plasmid containing the 1.8-kb insert in the sense orientation, was designated pSP64-MMTV-VimS (Fig. 2).

For use in cotransfection experiments, a plasmid designated pRGRN was constructed. pRGRN contains the rat glucocorticoid receptor cDNA and the neomycin phosphotransferase gene as separate transcription units, each under the control of the Rous sarcoma virus promoter. To construct pRGRN, the Bam HI site of the rat glucocorticoid receptor expression vector pRSVGR (Miesfeld et al., 1986) (gift of K. Yamamoto) was converted to an Mlu I site. The RSV promoter and glucocorticoid receptor gene were excised from the resulting vector by digestion with Mlu I. This Mlu I fragment was inserted into the plasmid pRSVneo (gift of B. Howard) at the unique Mlu I site to create pRGRN.

Cell Culture and DNA Transfection

HeLa cells (ATCC CCL 2.2) and SW-13 cells (ATCC CCL 105) were obtained from the American Type Culture Collection (Rockville, MD). MCF-7 cells were obtained from Dr. D. Edwards. Cells were grown in monolayer culture in a 1:1 mixture of Ham's F12:Dulbecco's MEM containing 5% FBS.

SW-13 cells express vimentin in a mosaic pattern (Hedberg and Chen, 1986). SW-13 cells were subcloned as described by Hedberg and Chen (1986). 50 subclones were obtained and examined for human vimentin content by immunofluorescence microscopy. 25 of the subclones were found to be essentially vimentin negative, 22 were mosaics with a significant number of positive and negative cells, and 3 subclones were obtained that appeared to contain essentially only cells with prominent vimentin filament networks. A subclone of the vimentin-positive cells, designated SW-13/cl.1 vim⁺ and vimentin negative cells, designated SW-13/cl.2 vim⁻ were selected for further study.

Stable cell lines were obtained by cotransfecting 0.6–0.8 × 10⁶ cells in 10-cm dishes with 40 μg pSP64-MMTV-VimS and 1.0 μg pRGRN by calcium phosphate precipitation (Graham and van der Eb, 1973) and 15% glycerol shock (Parker and Strak, 1979). Stable transfectants were selected in medium containing 400 μg/ml G-418. Individual colonies were recovered and examined for mouse vimentin filament content in the presence and absence of 10^{-7} M dexamethasone by indirect immunofluorescence. After 2–3 mo of continuous culture in 400 μg/ml G-418, stable cell lines were then maintained in medium containing 200 μg/ml G-418. Although preliminary experiments indicated that G-418 had no effect, all experiments were conducted in the absence of this antibiotic. Transient transfections were performed under similar conditions without cotransfection with pRGRN or G-418 selection.

Indirect Immunofluorescence

Cells were plated on sterile glass cover slips. The cells were rinsed briefly in PBS and then fixed in 70:30 acetone/methanol (vol/vol) at −20°C for 10 min. The cover slips were rinsed in PBS, and processed for indirect immunofluorescence as described by Franke et al. (1978). Rabbit anti-vimentin (Moscinski and Evans, 1987), and monoclonal anti-vimentin (V-9; Boehringer Mannheim Biochemicals, Indianapolis, IN) were used as primary antibodies. The rabbit anti-vimentin serum (diluted 1:100) visualized intermediate filaments in mouse cells, but did not detect filaments in a variety of vimentin containing human cells. Conversely, the commercial monoclonal anti-vimentin (2 μg/ml) visualized intermediate filaments in human cells but did not detect filaments in vimentin-containing mouse L-929 or 3T3 cells. Fluorescein-conjugated anti-rabbit and lissamine-rhodamine-conjugated anti-mouse antisera (Boehringer Mannheim Biochemicals) were used as second antibodies, respectively. All antibodies were diluted in PBS containing 1% ovalbumin and 1% normal goat serum. The cover slips were mounted in Aqua-mount (Lerner Laboratories, Pittsburgh, PA) and viewed on an Olympus microscope equipped with epifluorescence optics. Photographic exposures were made for 15–20 s using Kodak T-Max 400 film and the film processed with an exposure index of 1,200 using Kodak HC-110 developer. For all figures, the photographs represent identical exposures and photographic processing conditions.

Preparation and Analysis of [³⁵S]labeled Triton-insoluble Cytoskeletons

Cells were labeled with 25–50 μCi/ml [³⁵S]methionine for 2 h in methionine-free medium containing 1% FBS. Triton-insoluble cytoskeletons were prepared by the method of Zackroff and Goldman (1979) as previously described (Evans, 1984). In experiments with SW-13 cells, DNase I was de-

leted from the Triton-KCl solution to preserve filamentous actin as an internal marker. Triton-insoluble cytoskeletons were analyzed by one (Laemmli, 1970) and two-dimensional gel electrophoresis (O'Farrell, 1975). All second dimension SDS-PAGE contained 7.5% acrylamide. After electrophoresis, gels were stained with Coomassie blue and destained as previously described (Evans, 1984). The gels were dried and autoradiographed on Kodak XAR x-ray film at −70°C. In some experiments, [³⁵S]labeled proteins were directly quantitated in dried gels using an imaging scanner (System 200; Bioscan, Inc., Washington, DC). The gels were scanned for 20 min per lane using the two-dimensional analysis program. Background was subtracted using a nonradioactive portion of the gel. The [³⁵S] radioactivity for each gel lane and within individual protein peaks was determined using the manual mode.

Results

Expression of Murine Vimentin in Human Cells That Contain an Endogenous Vimentin Filament Network

HeLa cells contain an endogenous vimentin filament network in addition to keratin filaments (Moll et al., 1982; Quinlan et al., 1985) (Table I). Stable lines of HeLa cells transfected with the steroid-regulated vimentin expression plasmid were produced and screened for dexamethasone-dependent murine vimentin expression by immunofluorescence with an antibody specific for rodent vimentin. Fig. 3 shows double immunofluorescence of one transfectant cell line, HeLa/1C3, stained with rodent-specific (FITC) and human-specific (RITC) antivimentin antibodies with time after treatment with 10^{-7} M dexamethasone. There was no detectable expression of the transfected murine vimentin in the absence of dexamethasone and, as is common for cells in culture, the endogenous human vimentin filament staining pattern was nonuniform, with most cells exhibiting more concentrated vimentin filament staining in a perinuclear location (Fig. 3, A and B). 4–6 h after treatment with dexamethasone, many cells exhibited small focal patches of staining with the anti–mouse vimentin antibody, usually, but not always, in a perinuclear location (Fig. 3, C and D). Comparison of the location of the expressed mouse vimentin with the immunofluorescence staining pattern of the human vimentin filaments showed that the first detectable mouse protein always colocalized with the area of the most intense staining of the preexisting filament network. The mouse vimentin then appears to progressively colocalize with more peripheral areas of the human vimentin network until by 20 h after dexamethasone treatment, the mouse and human anti-vimentin immunofluorescence staining patterns were virtually identical (Fig. 3, G and H). These observations indicated that the expressed mouse vimentin is rapidly incorporated into the human filament network.

Table I. Intermediate Filament Proteins Expressed in Human Cell Lines Used in Vimentin cDNA Transfection Studies

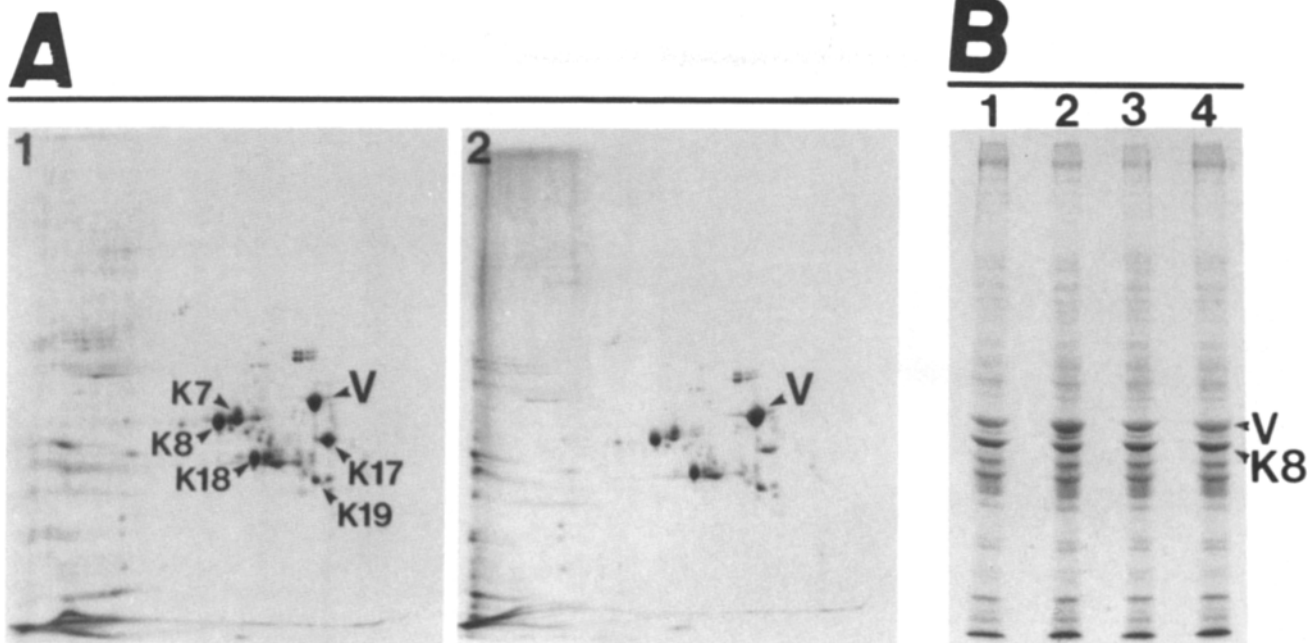|	Vimentin	Keratin
MCF-7	−	+
HeLa	+	+
SW-13/cl.1 vim⁺	+	−
SW-13/cl.2 vim⁻	−	−

556
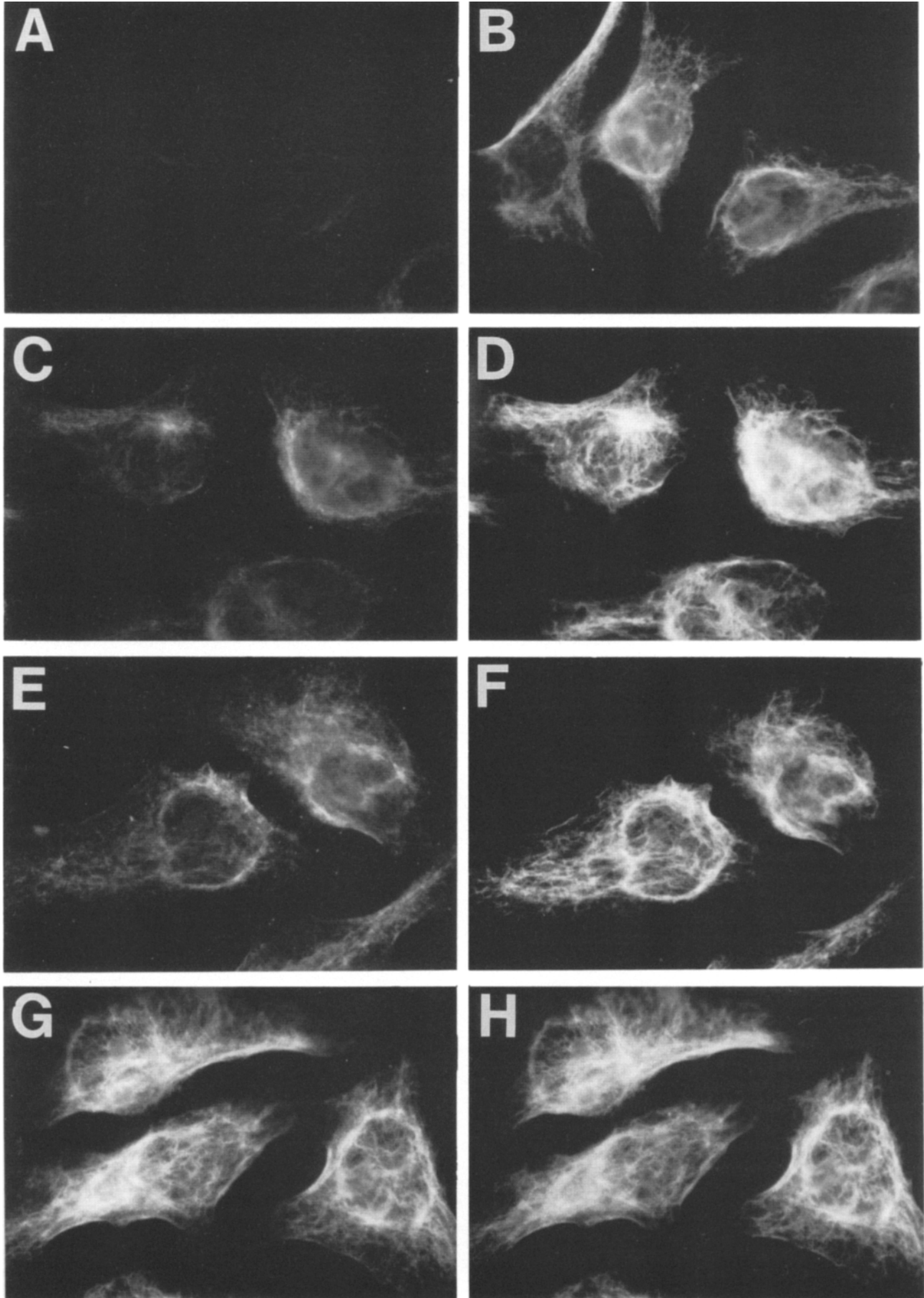
Figure 4. Polyacrylamide gel analysis of Triton-insoluble proteins from [^{35}S]methionine-labeled HeLa/IC3 cells. HeLa/IC3 and untransfected HeLa cells were cultured with or without 10^{-7} M dexamethasone for 24 h and then radiolabeled with [^{35}S]methionine for 2 h. Triton-insoluble cytoskeletons were prepared and analyzed by PAGE. The figure shows the ^{35}S autoradiographs. (*A*) Two-dimensional gel analysis of Triton-insoluble proteins from untreated (*1*) and dexamethasone-treated (*2*) HeLa/IC3 cells. (*B*) SDS-PAGE of untreated (lanes *1* and *3*) and dexamethasone treated (lanes *2* and *4*) HeLa/IC3 cells (lanes *1* and *2*) and untransfected HeLa cells (lanes *3* and *4*). The positions of vimentin (*V*) and cytokeratins (*K7, K8, K17, K18,* and *K19*) are indicated.

Previous studies have made similar observations of an initial perinuclear localization of newly synthesized (Albers and Fuchs, 1989) or microinjected (Vikstrom et al., 1989) intermediate filament proteins. These observations have been interpreted as indicating that the assembly–disassembly of intermediate filaments occurs as a polarized or vectorial process. However, if the assembly–disassembly of intermediate filament subunits with the preexisting human filament network was uniform per filament length, then the first place that newly synthesized mouse vimentin subunits would have been detectable would have been in areas of cytoplasm with the greatest concentration of filaments. Because the filaments are usually found in greatest concentration around the nucleus, it is difficult to differentiate between these two possibilities in these types of studies.

To demonstrate that the murine vimentin expressed in

Table II. Effect of Dexamethasone on Vimentin Synthesis in HeLa Cells Transfected with the Steroid Inducible Mouse Vimentin cDNA Vector

	HeLa/IC3						HeLa					
	[^{35}S]		Total*		V/K‡		[^{35}S]		Total		V/K‡	
	−	+	−	+	−	+	−	+	−	+	−	+
	cpm		%				*cpm*		%			
Vimentin	8,407	11,143	6.1	8.0			8,424	6,685	6.1	6.5		
Keratin-8	11,877	9,666	8.7	6.9	.7	1.2	13,893	11,381	9.9	7.6	.6	.6

HeLa/IC3 and untransfected HeLa cells were treated with dexamethasone, labeled with [^{35}S]methionine, and Triton-insoluble cytoskeletons prepared as described in Fig. 4. The [^{35}S]labeled proteins were separated by SDS-PAGE. One-dimensional polyacrylamide gels, including the gel used to produce the autoradiograph shown in Fig. 4 *B*, were directly scanned for [^{35}S] radioactivity as described in Materials and Methods. Values represent the average from duplicate SDS-gels obtained from the same experiment, (−) untreated and (+) dexamethasone treated.
* Percent total gel lane radioactivity in the indicated protein band.
‡ Ratio of vimentin to keratin-8 [^{35}S] radioactivity.

Figure 3. Expression of murine vimentin in HeLa/IC3 cells with time after induction with dexamethasone. HeLa/IC3 cells were obtained after stable transfection of HeLa cells with pSP64-MMTV-VimS and pRGRN. The figure shows double immunofluorescence staining patterns obtained with rabbit anti–mouse vimentin (FITC) (*A, C, E,* and *G*) and mouse monoclonal anti-human vimentin (RITC) (*B, D, F,* and *H*) antibodies for untreated cells (*A* and *B*), and cells 4 h (*C* and *D*), 8 h (*E* and *F*), and 20 h (*G* and *H*) after the addition of dexamethasone.
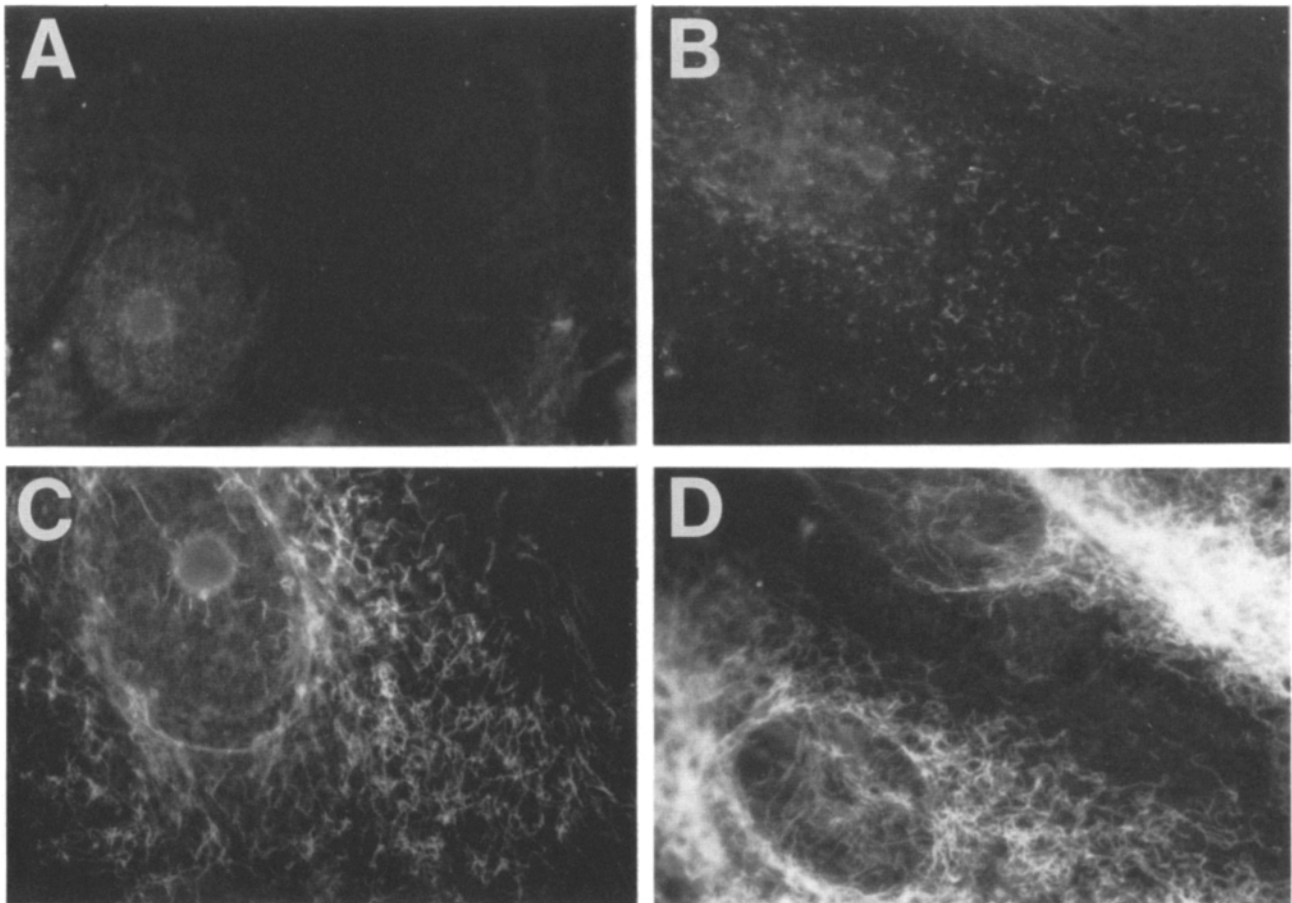
558
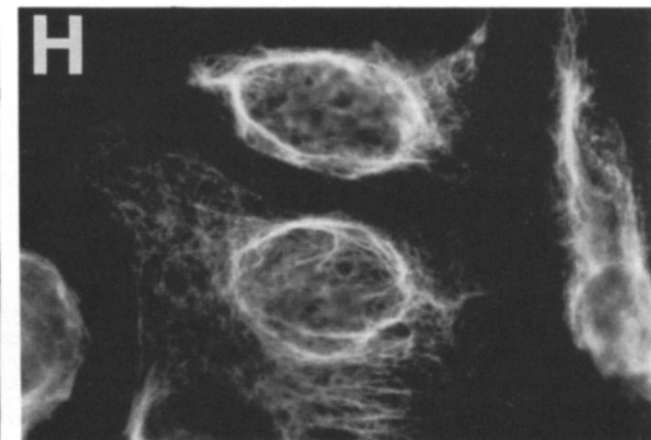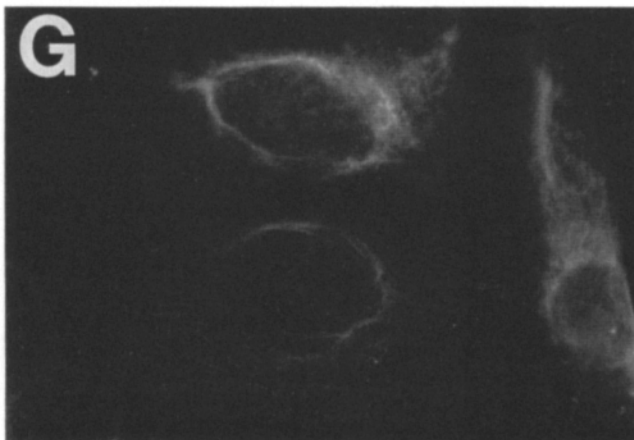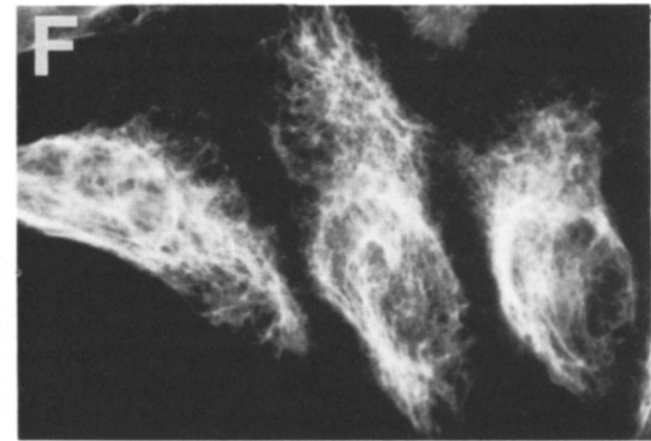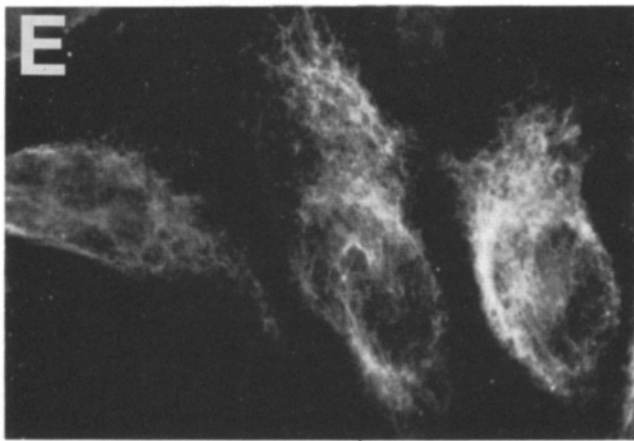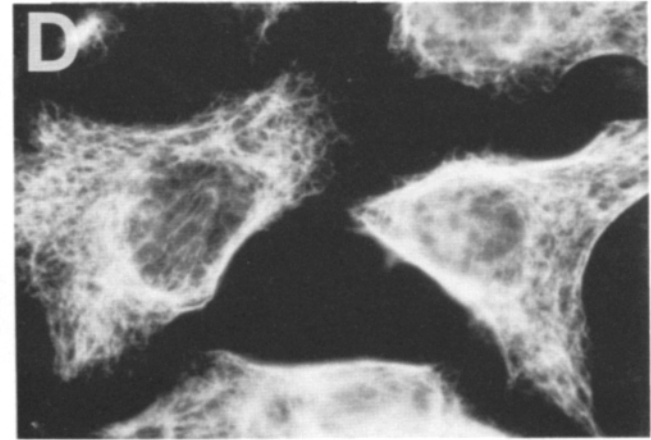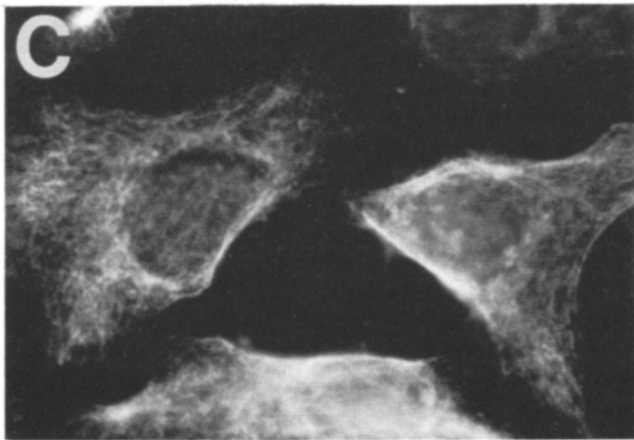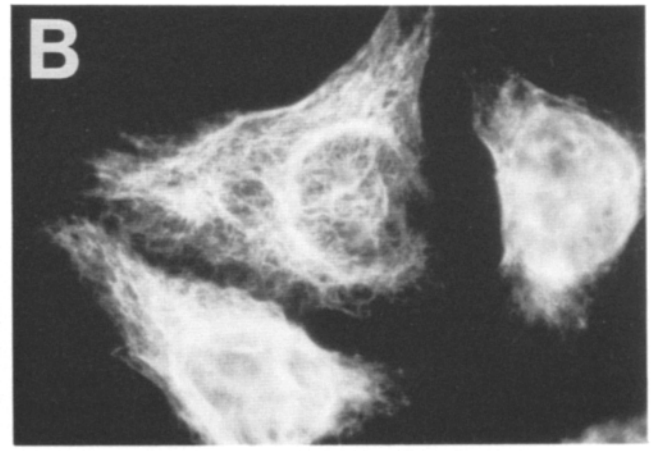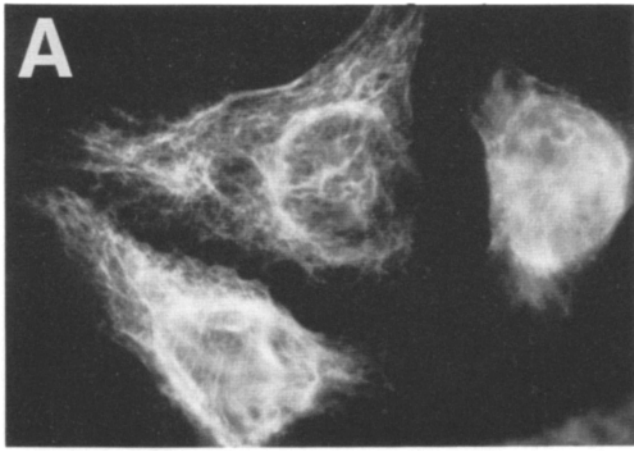
Figure 6. Expression of murine vimentin in MCF-7/1B2 cells with time after induction with dexamethasone. MCF-7/1B2 cells were obtained after stable transfection of MCF-7 cells with pSP64-MMTV-VimS and pRGRN. The figure shows the anti-mouse vimentin indirect immunofluorescence pattern of untreated cells (*A*), and cells 6 h (*B*), 8 h (*C*), and 24 h (*D*) after the addition of 10^{-7} M dexamethasone.

HeLa/1C3 cells was not an altered gene product and to gain some appreciation for the relative amount of species-specific vimentin produced in these cells, an analysis of [^{35}S]methionine-labeled Triton-insoluble cytoskeletons from untreated and dexamethasone treated HeLa/1C3 cells was performed. Preliminary studies had indicated that murine and human vimentin are indistinguishable on the basis of two-dimensional gel mobility, and that the anti-vimentin antisera that exhibit species specificity in immunofluorescence, cross-reacted in preliminary immunoblotting experiments. Furthermore, as shown in Fig. 4, dexamethasone treatment of the HeLa/1C3 cells for 24 h produced no obvious qualitative difference in the two-dimensional PAGE [^{35}S] autoradiograms of cell lysates or Triton-insoluble proteins compared with similar preparations from untreated cells. However, as shown in Table II, estimation of the amount of vimentin synthesis by direct quantitation of [^{35}S] Triton-insoluble proteins separated on SDS-PAGE, indicated that the relative amount of

vimentin synthesized during a 2-h pulse was selectively increased in HeLa 1C3 cells after dexamethasone treatment, compared to the rate of [^{35}S] incorporation into either cytokeratin proteins present in these preparations or total sample protein. Dexamethasone treatment appeared to actually decrease the relative incorporation of [^{35}S]methionine into keratin-8 in HeLa 1C3 cells and both vimentin and keratin-8 in untransfected HeLa controls (Table II). These experiments indicate that HeLa cells transfected with the murine vimentin cDNA vector can be induced to express a significant amount of murine vimentin that is indistinguishable from the endogenous human gene product on the basis of size and charge.

Loss of the Mouse Vimentin from the Vimentin Filament Network in HeLa/1C3 Cells after Removal of Dexamethasone

After removal of the inducer from HeLa/1C3 cell cultures,

Figure 5. Loss of the transfected mouse vimentin cDNA product from the endogenous vimentin filament network with time after removal of dexamethasone. HeLa/1C3 cells were treated with 10^{-7} M dexamethasone for 2 wk. The inducer was then removed from the growth medium (0 time) and cells cultured in the absence of dexamethasone. The figure shows the double immunofluorescence staining patterns obtained with rabbit anti-mouse vimentin (FITC) (*A, C, E,* and *G*) and mouse monoclonal anti-human vimentin (RITC) (*B, D, F,* and *H*) antibodies for cells at 0 time (*A* and *B*), 24 (*C* and *D*), 48 (*E* and *F*), and 72 h (*G* and *H*) after the removal of dexamethasone.
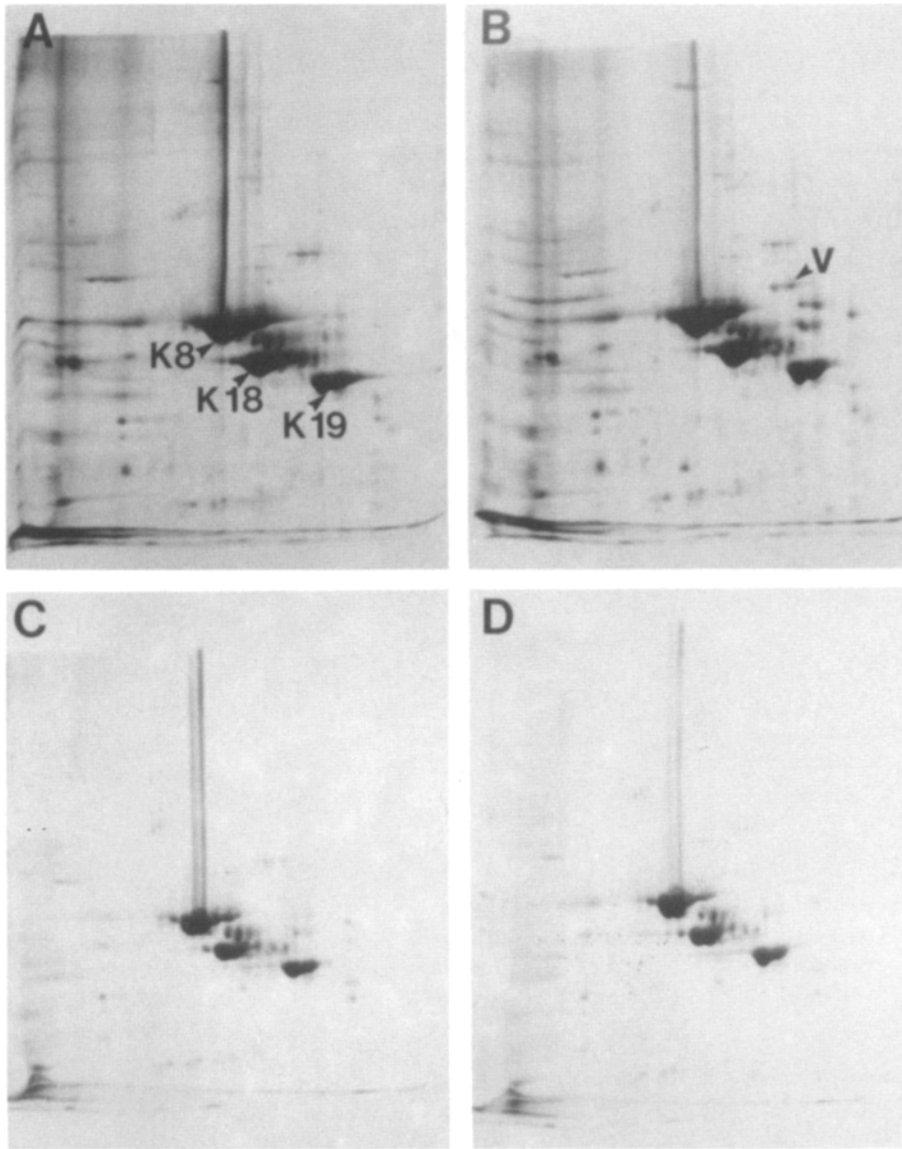
Figure 7. Two-dimensional gel analysis of Triton-insoluble proteins from [^{35}S]methionine labeled MCF-7 vimentin transfectants. The figure shows the autoradiograph of preparations from MCF-7/1B2 cells (*A* and *B*) and an MCF-7 transfectant clone that did not express detectable vimentin in immunofluorescence (*C* and *D*). Triton-insoluble proteins were prepared from cells that were untreated (*A* and *C*) and treated with 10^{-7} M dexamethasone (*B* and *D*). The positions of vimentin (*V*) and cytokeratins (*K8*, *K18*, and *K19*) are indicated.

the fate of the mouse vimentin that has been incorporated into the human network can be followed with time. If vimentin filament assembly is a polarized process directed outward from a perinuclear region, it would be anticipated that the mouse protein should appear to be lost initially from areas around the nucleus, as newly assembled human vimentin is incorporated, and should be last detected in more peripheral areas of the filament network. Conversely, if vimentin filament assembly is a more uniform process, then it would be anticipated that the mouse protein should appear to be lost initially from areas of human filament network with the least fluorescence intensity and should be last detected in areas of the human filament network with the greatest fluorescence intensity. Fig. 5 shows the anti–mouse and anti–human vimentin double immunofluorescence staining pattern of HeLa/1C3 cells with time after removal of dexamethasone. In this experiment, the cells had been cultured for 2 wk in the presence of 10^{-7} M dexamethasone and the mouse and human anti-vimentin immunofluorescence staining patterns were

identical (Fig. 5, *A* and *B*). After removal of the inducer, the intensity of the anti-mouse vimentin immunofluorescence slowly diminished, and by 48 h a visible loss, particularly from peripheral areas of the cytoplasm was apparent (Fig. 5, *E* and *F*). 72 h after removal of dexamethasone, many of the cells had little visible anti-mouse vimentin staining (Fig. 5, *G* and *H*). The last areas of visible fluorescence always co-localized with the most intensely stained area of the endogenous human filament network, usually, but not always, in a perinuclear location.

De Novo Vimentin Filament Assembly Occurs throughout the Cytoplasm When Murine Vimentin Is Expressed in Human Cells in the Absence of an Endogenous Vimentin Network

Human MCF-7 cells contain keratin filaments, but unlike most other epithelial cell lines in culture, do not express detectable levels of vimentin (Franke et al., 1983; Glass and
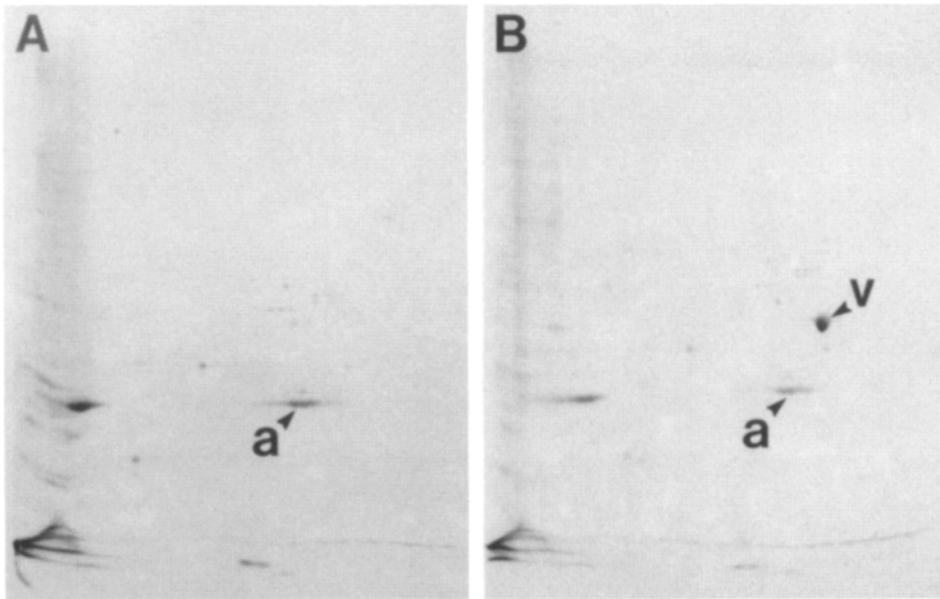
Figure 8. Two-dimensional gel analysis of Triton-insoluble proteins from [35S]methionine-labeled SW-13 cell subclones. The figure shows the [35S]autoradiograph of Cl.2 vim⁻ (*A*) and Cl.1 vim⁺ (*B*) cell preparations. The positions of actin (*a*) and vimentin (*v*) are indicated.

Fuchs, 1988) (Table I). Stable lines of MCF-7 cells transfected with the mouse vimentin expression plasmid were produced and screened by immunofluorescence with the anti-rodent vimentin antibody for the ability to express vimentin after induction with dexamethasone. Fig. 6 shows the anti-vimentin immunofluorescence staining of one transfectant line, MCF-7/2B1, with time after the induction of vimentin synthesis in the presence of 10^{-7} M dexamethasone. MCF-7/2B1 cells in the absence of dexamethasone did not contain detectable anti-vimentin immunofluorescence (Fig. 6 *A*). Within 6–8 h after the addition of dexamethasone, variable amounts of anti-vimentin reactive punctate or short filamentous structures became visible in the cytoplasm in many cells (Fig. 6 *B*). With increasing time after exposure to dexamethasone, cells exhibited progressively longer and more apparent filamentous cytoplasmic structures and by 24 h, some cells had anti-vimentin filament staining patterns that were not obviously different from other epithelial cells that express human vimentin filaments (Fig. 6 *D*). This de novo assembly of vimentin filaments appeared to occur throughout the cytoplasm of these cells, at least initially without any observable perinuclear localization. Similar results were obtained in experiments with a second transfectant MCF-7 line and in transient transfection experiments (data not shown). Expression of vimentin in MCF-7/1B2 cells had no obvious effect on the morphology or growth of these cells.

To confirm that the murine vimentin expressed in MCF-7 cells in response to dexamethasone was normal intermediate filament protein, cell lysates from untreated and dexamethasone treated [35S]methionine-labeled MCF-7/1B2 cells were analyzed by two-dimensional PAGE. As shown in Fig. 7, in the presence of dexamethasone, MCF-7/1B2 cells synthesized a protein with an identical two-dimensional PAGE mobility as murine vimentin. This protein was not found in untreated MCF-7/1B2 cells. This protein was also not detected in other stable, G418 resistant, MCF-7 transfectants that were vimentin negative in immunofluorescence, even in the

presence of the inducer (Fig. 7) or in untransfected MCF-7 cells in the presence or absence of dexamethasone (data not shown).

Expression of Murine Vimentin in Human SW-13 Cell Subclones That Either Contain or Lack Intermediate Filaments

Because the apparent differences in the assembly of expressed vimentin between HeLa and MCF-7 cells could simply be a reflection of comparing two dissimilar cell types, transfection experiments were also performed on subclones of the human adrenal carcinoma cell line SW-13 which either contain (SW-13/cl.1 vim⁺) or lack detectable vimentin filaments (SW-13/cl.2 vim⁻). Two-dimensional PAGE analysis of Triton-insoluble cytoskeletons prepared from [35S]methionine-labeled cells (Fig. 8) showed that in preparations from SW-13/cl.1 vim⁺ cells, vimentin was the most prominent protein detected, whereas in similar preparations from SW-13/cl.2 vim⁻ cells there was no detectable vimentin. Furthermore, relative to the amount of residual actin in these preparations, there were no other prominent labeled proteins that could be readily identified as intermediate filament proteins, with the exception of nuclear lamins. This is consistent with the previous observations of Hedberg and Chen (1986), that SW-13 cells do not contain other cytoplasmic intermediate filament types.

Both vim⁺ and vim⁻ cells were transiently transfected with pSP64-MMTV-VimS and the distribution of the expressed mouse vimentin examined with time after addition of dexamethasone as shown in Figs. 9 and 10. In SW-13/Cl.1⁺ cells, as in HeLa cells, the initial appearance of the mouse vimentin colocalized with the most intensely fluorescent area of the human filament network, usually in a perinuclear region of the cytoplasm, and then progressively colocalized with more peripheral areas of the endogenous filament network (Fig. 9). However, in transfected SW-13/Cl.2 vim⁻ cells, de novo filament assembly occurred
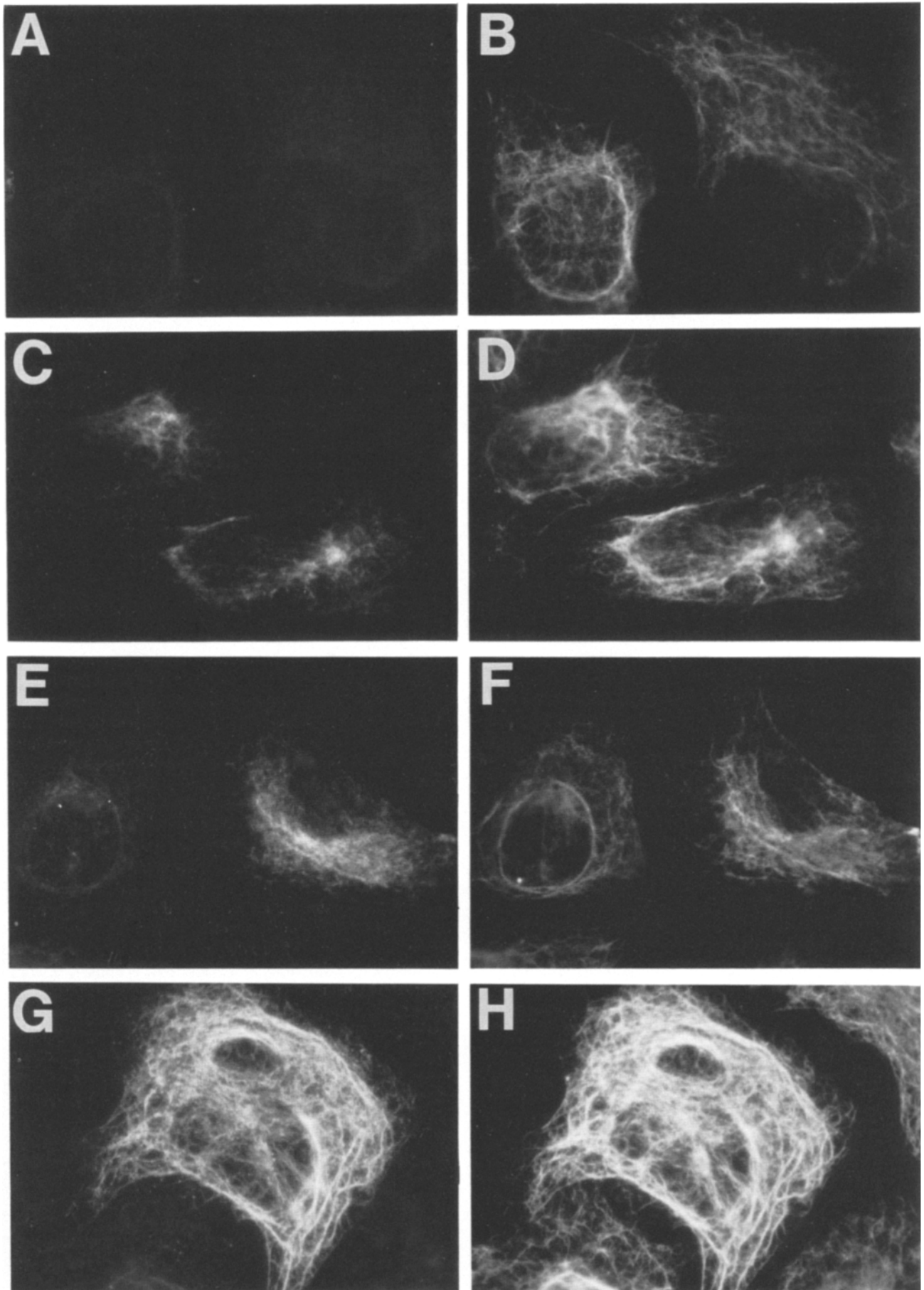
throughout the cytoplasm, similar to the vimentin filament assembly observed in MCF-7 cells (Fig. 10). These results indicated that the observed patterns of filament assembly are not a special property of a given cell type, but are general characteristics of cells that either contain or lack preexisting vimentin filaments.

Discussion

Examination of isolated intermediate filaments has generally indicated that the filaments lack polarity, that is, both ends of an individual filament are identical (Geisler et al., 1985; Stewart et al., 1989). The degree to which the incorporation and replacement of filament subunits occurs at filament ends or at internal sites along the filament is not clear, although Angelides et al. (1989) have recently reported kinetic studies on the neurofilament protein NF-L, indicating soluble subunits can exchange uniformly within filaments in vitro. Whereas intermediate filaments may not have a distinct physical polarity, Georgatos and Blobel (1987) have reported that different regions or domains of the subunit proteins could mediate interactions with nuclear and plasma membrane components in vitro, raising the possibility that filaments may have a functional polarity which could result in receptor mediated vectorial assembly.

Our studies demonstrate that in human HeLa and vimentin containing SW-13 cells transfected with a steroid-regulatable mouse vimentin cDNA expression plasmid, under induction conditions newly synthesized murine vimentin is first detected in the preexisting filament network in a nonuniform manner in indirect immunofluorescence microscopy. We have not observed the punctate localization of newly synthesized vimentin along the endogenous filaments that was observed by Ngai et al. (1990) in similar induction experiments. This phenomenon is similar to previous reports that biotinylated vimentin microinjected into cells (Vikstrom et al., 1989) or modified keratin cDNA transiently expressed in cells (Albers and Fuchs, 1989) results in immunofluorescence detection of the newly assembled proteins initially in the filament network in a perinuclear location and then progressively in filaments in more peripheral areas of the cytoplasm. We were concerned that nonuniformity in the distribution of the preexisting filaments in immunofluorescence microscopy could produce this effect.

Experiments with HeLa/IC3 cells to follow the localization of the mouse vimentin after removal of dexamethasone showed that the pattern of loss of the mouse protein from the human filament network was essentially the reverse of what was observed following synthesis of new protein. After the removal of the inducer, the last detectable mouse vimentin in these cells always corresponded to the most intensely fluorescent area of the human filament network, usually in a perinuclear area. The time course for the loss of mouse vimentin from these cells was considerably longer than the
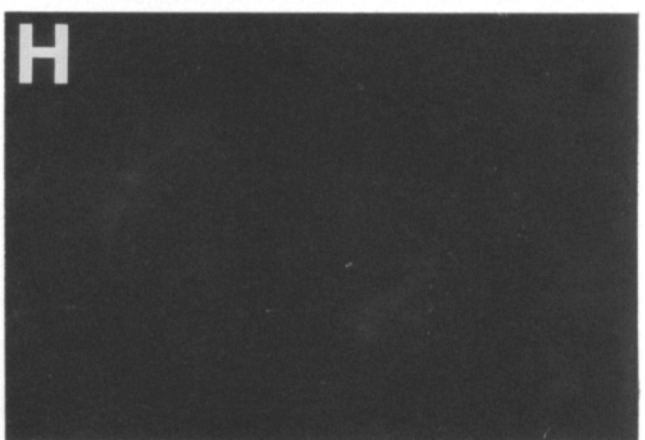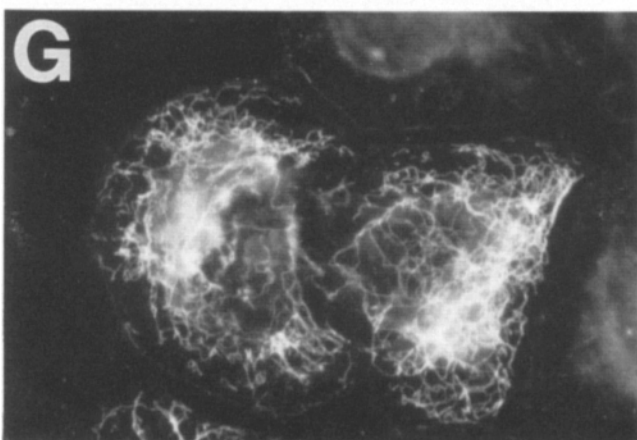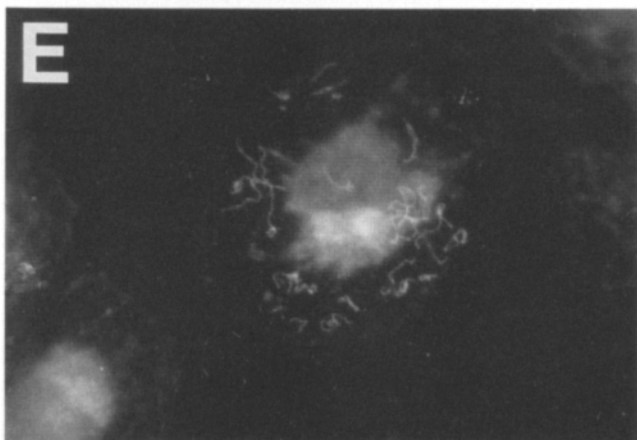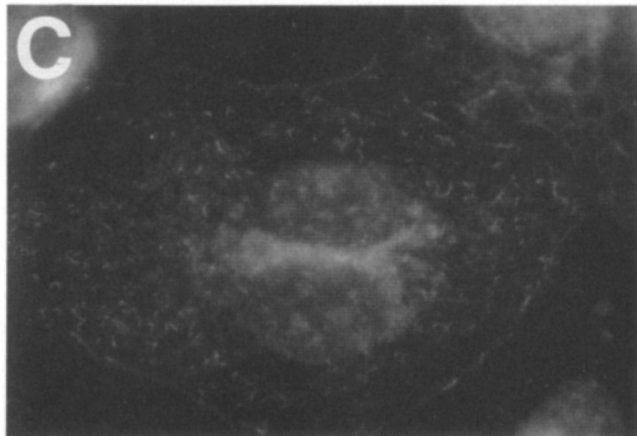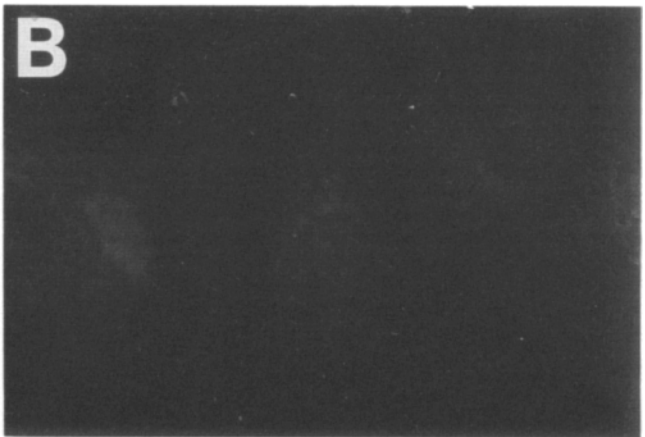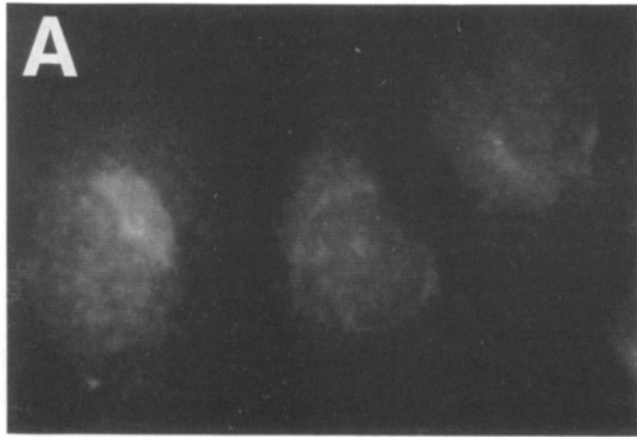
time required to observe newly synthesized protein under induction conditions. This result is compatible with the reported >6 h half-life for vimentin mRNA in cultured cells (Lilienbaum et al., 1986). These observations are most consistent with the dynamic incorporation and loss of intermediate filament protein throughout the length of the filaments, and suggest that the apparent perinuclear localization of newly synthesized vimentin in HeLa cells with preexisting vimentin networks could be due to nonuniformity in concentration of filaments in different areas of the cytoplasm in immunofluorescence microscopy. These experiments also indicate that vimentin filaments do not treadmill.

A fundamental difficulty in experiments that localize the incorporation of newly synthesized vimentin into an existing filament network is that these studies cannot differentiate between filament assembly and subunit protein turnover or exchange. In contrast to the pattern of appearance of newly synthesized vimentin in cells that contain preexisting vimentin-type filaments, de novo assembly of vimentin-type intermediate filaments can occur throughout the cytoplasm of MCF-7 and SW-13/cl.2 vim⁻ cells transfected with the mouse vimentin expression vector, at least initially without any discernable perinuclear localization. These observations are consistent with the mRNA microinjection experiments of Kreis et al. (1983), who found that de novo expression of keratin-type filaments resulted in filament assembly without a particular cytoplasmic localization. This would indicate that polarized or vectorial assembly from a perinuclear region into more peripheral areas of the cytoplasm is clearly not a requirement to assemble intermediate filaments in vivo.

These results would seem to be most consistent with a model of relatively uniform and dynamic intermediate filament assembly throughout the cytoplasm. These experiments do not formally eliminate the possibility that filament assembly could occur as a result of a recycling-type mechanism, although in light of current models of intermediate filament structure this would seem unlikely. These studies do indicate that this question needs to be more critically evaluated at a level of resolution that eliminates the relatively two dimensional nature of fluorescence microscopy. In addition, these experiments do not address the nature of filament interactions with specific nuclear or plasma membrane components. The formation of specific interactions between intermediate filaments and other cellular structures may be independent of the symmetry of the assembly process. Regardless of the precise nature of the assembly process, these observations are consistent with other recent studies (Albers and Fuchs, 1987; 1989; Vikstrom et al., 1989), indicating that intermediate filaments are more dynamic structures than previously supposed.

Figure 9. Expression of murine vimentin in a SW-13 cell subclone (Cl.1 vim⁺) that contains human vimentin filaments with time after transfection and addition of dexamethasone. The cells were transiently transfected with pSP64-MMTV-VimS. 24 h after transfection, the cells were treated with 10⁻⁷ M dexamethasone. The figure shows double immunofluorescence of cells at 0 time (A and B), 6 (C and D), 8 (E and F), and 20 h (G and H) after the addition of dexamethasone, with rabbit anti-mouse vimentin (FITC) (A, C, E, and G) and mouse monoclonal anti-human vimentin (RITC) (B, D, F, and H) antibodies.

References

Albers, K., and E. Fuchs. 1987. The expression of mutant epidermal keratin cDNAs transfected in simple epithelial and squamous cell carcinoma lines. *J. Cell Biol.* 105:791-806.

Albers, K., and E. Fuchs. 1989. Expression of mutant keratin cDNAs in epithelial cells reveals possible mechanisms for initiation and assembly of intermediate filaments. *J. Cell Biol.* 108:1477-1493.

Angelides, K. L., K. E. Smith, and M. Takeda. 1989. Assembly and exchange of intermediate filament proteins of neurons: neurofilaments are dynamic structures. *J. Cell Biol.* 108:1495-1506.

Blikstad, I., and E. Lazarides. 1983. Vimentin filaments are assembled from a soluble precursor in avian erythroid cells. *J. Cell Biol.* 96:1803-1808.

Eckert, B. S., and S. E. Caputi. 1985. Relation of the intermediate filament distribution center to keratin filament dynamics *in vivo*: cells at the edge of an experimental wound. *Ann. NY Acad. Sci.* 455:343-353.

Eckert, B. S., R. A. Daley, and L. M. Parysek. 1982a. Assembly of keratin onto PtK1 cytoskeletons: evidence for an intermediate filament organizing center. *J. Cell Biol.* 92:575-578.

Eckert, B. S., R. A. Daley, and L. M. Parysek. 1982b. *In vivo* disruption of the cytoskeleton in cultured epithelial cells by microinjection of antikeratin: evidence for the presence of an intermediate filament organizing center. *Cold Spring Harbor Symp. Quant. Biol.* 46:403-412.

Evans, R. M. 1984. Peptide mapping of phosphorylated vimentin. Evidence for a site-specific alteration in mitotic cells. *J. Biol. Chem.* 259:5372-5375.

Franke, W. W., E. Schmid, M. Osborn, and K. Weber. 1978. Different intermediate-sized filaments distinguished by immunofluorescence microscopy. *Proc. Natl. Acad. Sci. USA.* 75:5034-5038.

Franke, W. W., E. Schmid, and R. Moll. 1983. The intermediate filament cytoskeleton in tissues and in cultured cells: differentiation specificity of expression of cell architectural elements. *In* Human Carcinogenesis. C. C. Harris, and H. N. Autrup, editors. Academic Press, Orlando, FL. 3-34.

Franke, W. W., E. Schmid, S. Mittnacht, C. Grund, and J. L. Jorcano. 1984. Integration of different keratins into the same filament system after microinjection of mRNA for epidermal keratins into kidney epithelial cells. *Cell.* 36:813-825.

Geisler, N., F. Kaufmann, and K. Weber. 1985. Antiparallel orientation of the two double-stranded coiled-coils in the tetrameric protofilament unit of intermediate filaments. *J. Mol. Biol.* 182:173-177.

Georgatos, S. D., and G. Blobel. 1987. Two distinct attachment sites for vimentin along the plasma membrane and the nuclear envelope in avian erythrocytes: a basis for a vectorial assembly of intermediate filaments. *J. Cell Biol.* 105:105-115.

Glass, C., and E. Fuchs. 1988. Isolation, sequence, and differential expression of a human K7 gene in simple epithelial cells. *J. Cell Biol.* 107:1337-1350.

Goldman, R., A. Goldman, K. Green, J. Jones, N. Lieska, and H.-K. Yang. 1985. Intermediate.filaments: possible functions as links between the nucleus and cell surface. *Ann. NY Acad. Sci.* 455:1-17.

Goldman, R. D., A. E. Goldman, K. G. Green, J. C. R. Jones, S. M. Jones, and H.-Y. Yang. 1986. Intermediate filament networks: organization and possible functions of a diverse group of cytoskeletal elements. *J. Cell Sci. Suppl.* 5:69-97.

Graham, F. L., and A. J. van der Eb. 1973. A new technique for the assay of infectivity of human adenovirus 5 DNA. *Virology.* 52:456-467.

Han, J. H., C. Stratowa, and W. J. Rutter. 1987. Isolation of full-length putative rat lysophospholipase cDNA using improved methods for mRNA isolation and cDNA cloning. *Biochemistry.* 26:1617-1624.

Hedberg, K. K., and L. B. Chen. 1986. Absence of intermediate filaments in a human adrenal cortex carcinoma derived cell line. *Exp. Cell Res.* 163:509-517.

Klymkowsky, M. W., J. B. Bachant, and A. Domingo. 1989. Functions of intermediate filaments. *Cell Motil. Cytoskel.* 14:309-331.

Kreis, T. E., B. Geiger, E. Schmid, J. L. Jorcano, and W. W. Franke. 1983. De novo synthesis and specific assembly of keratin filaments in nonepithelial cells after microinjection of mRNA for epidermal keratin. *Cell.* 32:1125-1137.

Laemmli, U. K. 1970. Cleavage of structural proteins during the assembly of the head of bacteriophage T4. *Nature (Lond.).* 227:680-685.

Lilienbaum, A., U. Legagneux, M.-M. Portier, K. Dellagi, and D. Paulin. 1986. Vimentin gene expression in human lymphocytes and in Burkitt's lymphoma cells. *EMBO (Eur. Mol. Biol. Organ.) J.* 5:2809-2814.

Miesfeld, R., S. Rusconi, P. J. Godowski, B. A. Maler, S. Okret, A.-C. Wikstrom, J.-A. Gustafsson, and K. R. Yamamoto. 1986. Genetic complementation of a glucocorticoid receptor deficiency by expression of cloned receptor cDNA. *Cell.* 46:389-399.

Moll, R., W. W. Franke, D. L. Schiller, B. Geiger, and R. Krepler. 1982. The catalog of human cytokeratins: patterns of expression in normal epithelia, tumors and cultured cells. *Cell.* 31:11-24.

Moscinski, L. M., and R. M. Evans. 1987. Changes in the organization of vimentin-type intermediate filaments during retinoic acid induced differentiation of embryonal carcinoma cells. *In* International Symposium on the Cytoskeleton in Differentiation and Development. J. Arechaga, and R. Maccioni, editors. ICSU Press, 267-279.

Ngai, J., T. R. Coleman, and E. Lazarides. 1990. Localization of newly synthesized vimentin subunits reveals a novel mechanism of intermediate filament assembly. *Cell.* 60:415-427.

O'Farrell, P. H. 1975. High resolution two-dimensional electrophoresis of proteins. *J. Biol. Chem.* 250:4007-4021.

Parker, B. A., and G. R. Stark. 1979. Regulation of simian virus 40 transcription: sensitive analysis of the RNA species present early in infections by virus or viral DNA. *J. Virol.* 31:360-369.

Quax, W., W. V. Egberts, W. Hendricks, Y. Quax-Jeuken, and H. Bloemendal. 1983. The structure of the vimentin gene. *Cell.* 35:215-223.

Quax-Jeuken, Y., W. Quax, and H. Bloemendal. 1983. Primary and secondary structure of hamster vimentin predicted from the nucleotide sequence. *Proc. Natl. Acad. Sci. USA.* 80:3548-3552.

Quinlan, R. A., D. L. Schiller, M. Hatzfeld, T. Achtstatter, R. Moll, J. L. Jorcano, T. M. Magin, and W. W. Franke. 1985. Patterns of expression and organization for cytokeratin intermediate filaments. *Ann. NY Acad. Sci.* 455:282-306.

Robson, R. M. 1989. Intermediate filaments. *Curr. Op. Cell Biol.* 1:36-43.

Sarria, A. J., and R. M. Evans. 1989. Intermediate filaments in biology and disease. *RBC Cell Biol. Rev.* 22:1-77.

Soellner, P., R. A. Quinlan, and W. W. Franke. 1985. Identification of a distinct soluble subunit of an intermediate filament protein: tetrameric vimentin from living cells. *Proc. Natl. Acad. Sci. USA.* 82:7929-7933.

Steinert, P. M., and R. Roop. 1988. Cellular and molecular biology of intermediate filaments. *Annu. Rev. Biochem.* 57:593-625.

Stewart, M., R. A. Quinlan, and R. D. Moir. 1989. Molecular interactions in paracrystals of a fragment corresponding to the α-helical coiled-coil rod portion of glial fibrillary acidic protein: evidence for an antiparallel packing of molecules and polymorphism related to intermediate filament structure. *J. Cell Biol.* 109:225-234.

Vikstrom, K. L., G. G. Borisy, and R. D. Goldman. 1989. Dynamic aspects of intermediate filament networks in BHK-21 cells. *Proc. Natl. Acad. Sci. USA.* 86:549-553.

Zackroff, R. V., and R. D. Goldman. 1979. *In vitro* assembly of intermediate filaments from baby hamster kidney (BHK-21) cells. *Proc. Natl. Acad. Sci. USA.* 76:6226-6230.

Figure 10. Expression of murine vimentin in a SW-13 cell subclone (Cl.2 vim⁻) that lacks human vimentin filaments with time after transfection and addition of dexamethasone. The cells were transiently transfected with pSP64-MMTV-VimS. 24 h after transfection, the cells were treated with 10^{-7} M dexamethasone. The figure shows double immunofluorescence of cells at 0 time (*A* and *B*), 6 (*C* and *D*), 8 (*E* and *F*) and 20 h (*G* and *H*) after the addition of dexamethasone, with rabbit anti-mouse vimentin (FITC) (*A, C, E,* and *G*) and mouse monoclonal anti-human vimentin (RITC) (*B, D, F,* and *H*) antibodies.